JOURNAL OF MATERIALS SCIENCE 16 (1981) 2439–2448

Investigation of the vaterite–calcite transformation by ESR spectroscopy using Mn^{2+} ions as a tracer

B. FUBINI*, F. S. STONE
School of Chemistry, University of Bath, Bath, UK

Vaterite ($CaCO_3$) containing 50 ppm Mn^{2+} as an electron spin resonance (ESR) tracer has been subjected to various heat treatments at temperatures up to 500° C in order to monitor the transformation to calcite. Samples have been examined both by X-ray powder diffraction and ESR spectroscopy and the results from the two techniques are correlated. In contrast to the smeared ESR signal in vaterite, the sharp ESR spectrum of Mn-doped calcite enables its crystallization to be followed, and it is shown that the transformation occurs progressively. There is no sharp transition temperature, although the rate becomes very rapid at 400° C. The ESR spectum of polycrystalline calcite prepared from vaterite shows differences of detail from that of calcite precipitated at room temperature, notably in respect of a strong signal at $\theta = 0°$ and a weaker response from transitions other than $M = \frac{1}{2} \leftrightarrow M = -\frac{1}{2}$. These features are attributed to variations in the axial field parameter D for the paramagnetic Mn ions in the sample.

1. Introduction

Calcium carbonate is known in three crystalline modifications, namely calcite, aragonite and vaterite. Calcite is the thermodynamically stable form at room temperature, but aragonite and vaterite can be obtained as metastable forms. Many factors influence the formation of the individual polymorphs, notably supersaturation [1], temperature [2], CO_2 partial pressure [2], mechanical pressure [3] and the presence of foreign ions [4–7].

In this paper we are concerned with calcite and vaterite. These polymorphs differ in various properties [8–11], but the main structural distinction is that the planes of the carbonate groups are perpendicular to the c-axis in calcite and parallel to it in vaterite, and as a result the co-ordination of the Ca^{2+} ion is different in the two modifications.

At room temperature vaterite can be transformed irreversibly into calcite on digestion in aqueous media. It is also transformed into calcite by thermal treatment in the dry state. However, the temperature of transition is not clearly defined. Values in the range 375 to 400° C have been quoted [12, 13] but Rao [14] has reported that the rate of transformation is immeasurably low below 450° C. Turnbull [15] has recently made a detailed thermochemical study of vaterite. He considers that the discrepancies regarding the transformation to calcite can be ascribed to different levels of impurities and to variations in excess energy arising from small crystallite size and from lattice disorder and distortion [16].

The calcium ions in vaterite are in a distorted 8-fold co-ordination with oxygen, but in calcite, with its higher symmetry, the co-ordination of calcium with oxygen is 6-fold octahedral. In view of this distinction, we considered that it should be possible to obtain useful information about the transformation by means of Mn^{2+} as an ESR tracer, the hyperfine structure being definitive for a high-symmetry crystal field [17–19].

Mn^{2+} in calcite single crystals has been extensively studied by ESR [20–29]. Brief attention

*On leave from the Institute of General and Inorganic Chemistry, Faculty of Pharmacy, University of Turin, Italy.

0022–2461/81/092439–10$03.00/0

has also been paid to crushed single crystals and microcrystalline calcite [20, 30, 31]. Since the vaterite–calcite transformation has necessarily to be studied on powdered samples, it was important for the present work that the ESR spectrum of powdered Mn^{2+}–calcite should be investigated. We therefore report in this paper on the spectrum of Mn^{2+} in polycrystalline calcite and vaterite as well as on variously heated vaterite samples in relation to the vaterite → calcite transition.

An X-ray powder diffraction study of the transition is also reported and correlated with the ESR work.

2. Experimental procedures

2.1. Preparation of Mn-doped calcite and vaterite

Mn-doped calcite (100 ppm Mn) samples were obtained by slowly dripping a solution of 0.2M $Ca(NO_3)_2$ containing the appropriate amount of $Mn(NO_3)_2$ into a 0.5M $(NH_4)_2CO_3$ solution at room temperature. Nitrogen was bubbled through the solution during precipitation and the filtered precipitate was washed with water under the protection of a CO_2 layer (obtained by having dry ice in the filter funnel) in order to avoid any oxidation of the Mn^{2+} ions. Prolonged contact with the mother liquor is known to favour the formation of calcite.

Mn-doped vaterite samples were prepared by the same precipitation procedure but favouring the formation of vaterite by carrying out the operations at 60° C [1], washing the preciptate with ethanol instead of water and by lowering the Mn^{2+} content to 50 ppm. The vaterite samples contained only a very small proportion of calcite. X-ray diffraction analysis showed that the vaterite phase so obtained was stable for at least one year at room temperature.

A sample of Mn-doped calcite (10 ppm) was also prepared in order to have calcites with higher and lower manganese content than the vaterite samples.

Samples prepared by the above procedures have been found to have surface areas (determined by N_2 adsorption at 77 K) of 25 to 30 $m^2\ g^{-1}$, indicative of a mean particle size, assuming low porosity, of about 100 nm.

2.2. Techniques

X-ray diffraction analysis was performed by the Debye–Scherrer method using a 114.6 mm diameter camera and CuKα radiation. Samples were placed in 0.5 mm Lindemann glass capillary tubes. Optical density measurements of X-ray films were performed with a Joyce Loebel recording microdensitometer.

ESR spectra were recorded with a Varian E-3 spectrometer using *X*-band (9.53 GHz) radiation. All spectra were recorded at room temperature and in air; however, no changes in the Mn^{2+} spectrum in $CaCO_3$ were found when recorded under vacuum. In order to obtain undistorted line shapes, low values of modulation amplitude (< 0.5 G) were used. The microwave power was kept as low as possible to avoid saturation.

2.2.1. Procedure for transformation of vaterite

Mn-doped vaterite (50 ppm Mn) was heated in a furnace for successive periods of about 3 h at temperatures of 300, 380, 410 and 430° C, with cooling after each period. The resulting solids will be referred to as Vat 1, Vat 2, Vat 3 and Vat 4, respectively. Vat 0 indicates the untreated sample. In order to be sure that the transformation to calcite was complete after 3 h at 430° C, one additional long period of heating (20 h) was performed at 500° C (Vat 5). A further thermal treatment at 600° C initiated calcite decomposition.

X-ray diffraction and ESR measurements were made on cooling to room temperature after each thermal treatment.

3. Results

3.1. X-ray diffraction analysis

3.1.1. Calcite

X-ray diffraction patterns from the calcite samples were characteristic of well-crystallized calcite and showed no lines from other $CaCO_3$ polymorphs.

3.1.2. Vaterite

Vat 0 exhibited the diffraction pattern of vaterite, with some very feeble lines from calcite. This is usual for laboratory preparations of vaterite. To determine the amount of calcite (and also to determine the amounts of calcite in Vat 1 to 5), a calibration curve was constructed [32]. Weighed amounts of calcite were added to the most pure vaterite obtainable (gannet egg shells) [33], and the relative peak intensities of the calcite (1 0 4) and vaterite (1 1 2) lines were measured. The calibration curve is shown by the continuous line in Fig. 1. In this way the amount of calcite in Vat 0 was evaluated to be 5% or less.

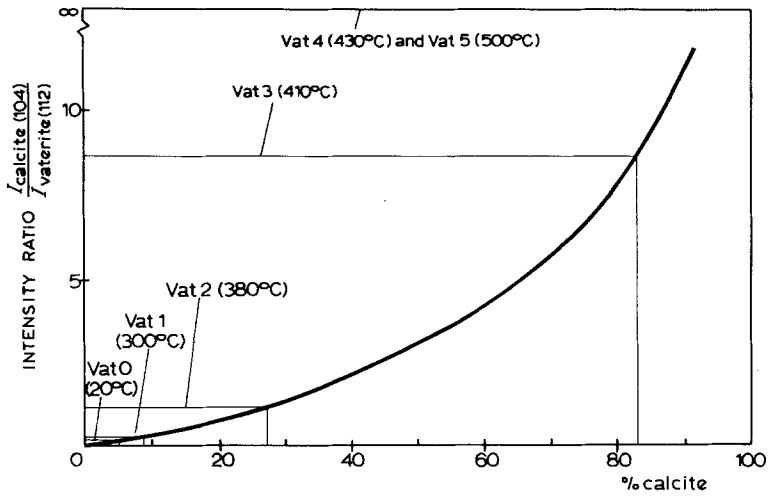

Figure 1 Evaluation by X-ray diffraction of the calcite content of vaterite samples heated to different temperatures. The solid curve is a calibration curve obtained using known mixtures.

The development of calcite from vaterite by thermal treatment is illustrated in Fig. 1, where intensity ratios for Vat 0, Vat 1, Vat 2 and Vat 3 are indicated. Using the calibration curve it is then seen that a progressive transformation into calcite occurs in these finely divided materials. An increase in the amount of calcite is detectable already at 300° C, far below the stated transformation temperatures [12–14]. With the heating intervals chosen (3 h), the largest change occurs between 380 and 410° C. However, there is no evidence of an abrupt transformation. X-ray patterns from Vat 4 and Vat 5 were identical to those from the prepared calcite samples, and all lines of vaterite were absent ($I_{calcite(104)}/I_{vaterite(112)} = \infty$). The transformation is therefore complete at 430°C.

3.2. ESR spectra

3.2.1. Mn^{2+} in polycrystalline calcite

The ESR spectrum from divalent manganese in calcite (100 ppm) is shown in Fig. 2. The spectrum

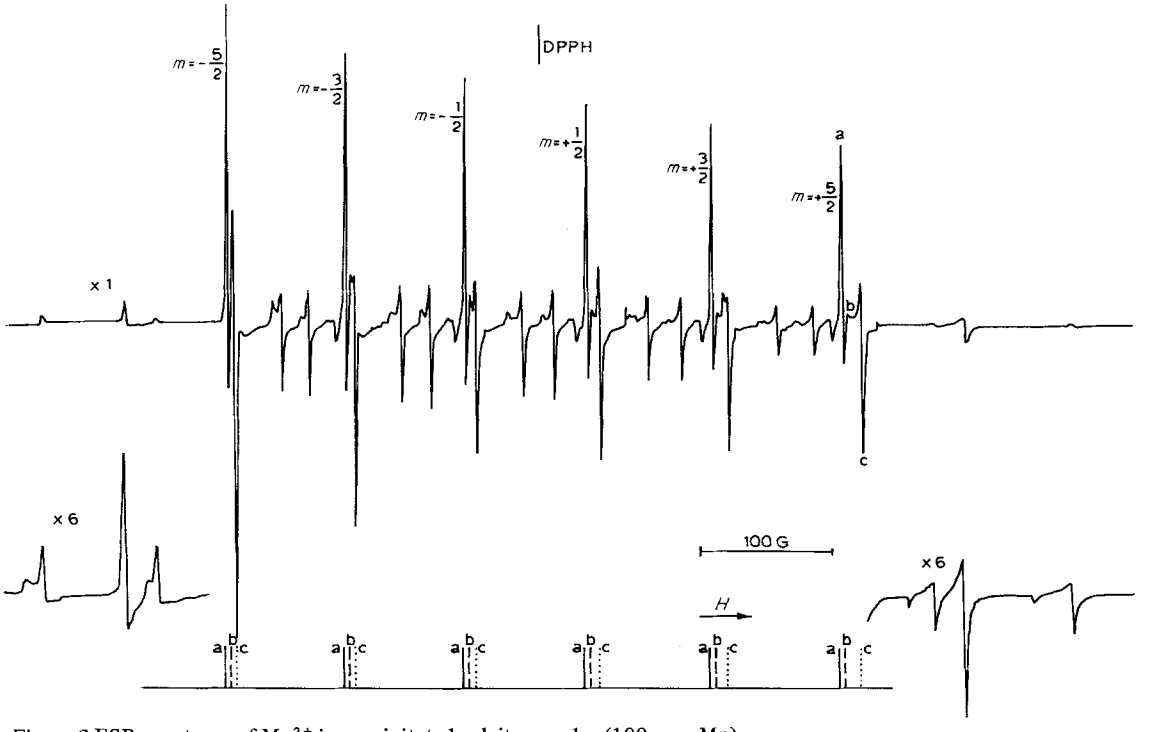

Figure 2 ESR spectrum of Mn^{2+} in precipitated calcite powder (100 ppm Mn).

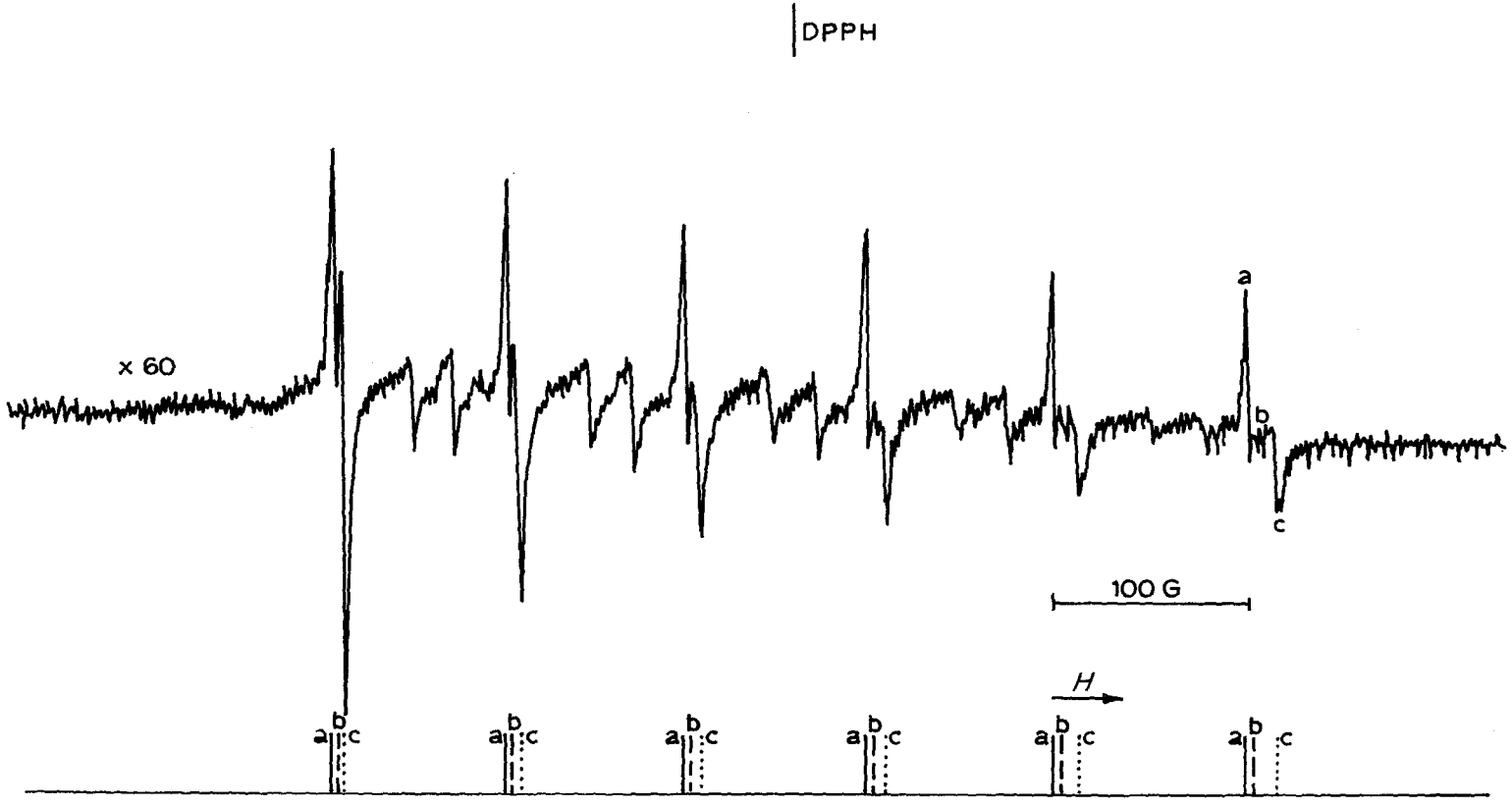

Figure 3 ESR spectrum of Mn^{2+} in precipitated vaterite powder (calcite < 5%). Magnification (× 60) is with respect to the calcite spectrum of Fig. 2.

from the sample with the lower Mn^{2+} content (10 ppm) is the same, except for the intensity of the lines, and therefore is not reported. No change in the spectrum occurred when the samples were heated.

The major features of the spectrum are two sextuplets of lines, close to each other, indicated in Fig. 2 as "a" (solid line) and "c" (dotted line), whose components have comparable intensity. The spacing between the "a" components and the spacing between the "c" components both increase with increasing field, the effect being more marked with the "c" components. Between "a" and "c" lines are components of another, but very weak, sextuplet, indicated in Fig. 2 as "b" (dashed line), whose spacings are the same as for the "a" sextuplet. Not all six lines of the "b" sextuplet are visible because of the overlap with the "c" sextuplet at the low field end. Finally, in each of the five ranges between the sextuplet components a pair of weaker lines occurs.

Minor features are weak lines both between the sextuplet components and outside them. The weak lines falling in the outer parts of the spectrum are shown in Fig. 2 at higher amplification.

The spectrum differs from that reported for crushed single crystals [20, 30, 31] in respect of the presence of sextuplet "b" and a much more detailed set of weak lines, both outer and inner.

3.2.2. Mn^{2+} in polycrystalline vaterite

Fig. 3 shows the ESR spectrum due to 50 ppm Mn^{2+} in vaterite (Vat 0). The overall intensity of the spectrum is very low (only a few per cent of that of a calcite sample with the same Mn^{2+} content) and a particularly high amplification (× 60) was needed to record it. Despite this fact, it is possible to observe that all the lines in Fig. 3 coincide in position with the major lines in Fig. 2 and that no new lines are detectable. The spectrum in Fig. 3 is therefore consistent with a conclusion that there are traces of Mn-containing calcite present in the vaterite sample but that the characteristic spectrum of Mn^{2+} in vaterite *per se* is not observable on account of the low site symmetry leading to a completely broadened signal. Changes in the ESR spectrum on heating can therefore be used specifically to observe the growth of calcite.

3.2.3. Mn^{2+} spectra during vaterite–calcite transformation

Beginning with Vat 0, each thermal treatment up to 430° C caused an increase in the overall intensity of the spectrum, and a further but slight increase occurred also above this temperature. However, the line positions and the relative intensities of the lines are all the same. The most intense (Vat 5) is shown in Fig. 4.

The Vat 5 spectrum of Fig. 4 (and those of Vat 0 to 4) are basically similar to that of Mn^{2+} in directly precipitated calcite shown in Fig 2, but there are some differences in the relative intensities of the lines. We comment on this in the next section.

All spectra were obtained under identical conditions, so that we may assume, as a rough measure of the overall intensity, the height of the $m = 5/2$ peak. Although a double integration of the signals would yield a more accurate measure of the intensity, the peak height can be assumed as an intensity measure when, as in the present case, the shape and linewidth of the peak remains unaltered. The variation of this intensity along the series Vat 0 → Vat 5 is reported in Fig. 5a as a function of heating temperature. In Fig. 5b the intensity is plotted against the percentage of calcite, using data for the latter evaluated from Fig. 1.

Taking into account the inaccuracies inherent in both the X-ray diffraction and ESR intensity measurements, Fig. 5b shows a very satisfactory proportionality between ESR intensity and percentage conversion. This relationship further supports the conclusion that Mn^{2+} ions are exhibiting a structured ESR signal only in the calcite phase.

The intensity against temperature curve (Fig. 5a) is sigmoidal, with a point of inflection at about 410° C. The Vat 5 value, which was obtained after prolonged heating at 500° C, can be considered as a limiting value, but it should be borne in mind that the intensity may rise between Vat 4 and Vat 5 due to slow surface crystallization in the calcite phase rendering more of the Mn^{2+} ions in that phase visible by ESR.

3.2.4. Mn^{2+} in calcite from vaterite

As already stated, the spectrum of Vat 5 (Fig. 4) is basically the same as the calcite spectrum (Fig. 2). However, three main differences may be discerned:

(i) the sextuplet "b" is definitely more intense in calcite ex vaterite (Fig. 4) than in directly precipitated calcite (Fig. 2);

(ii) the fine structure lines (compare the outer parts of Figs 2 and 4) are extremely weak in cal-

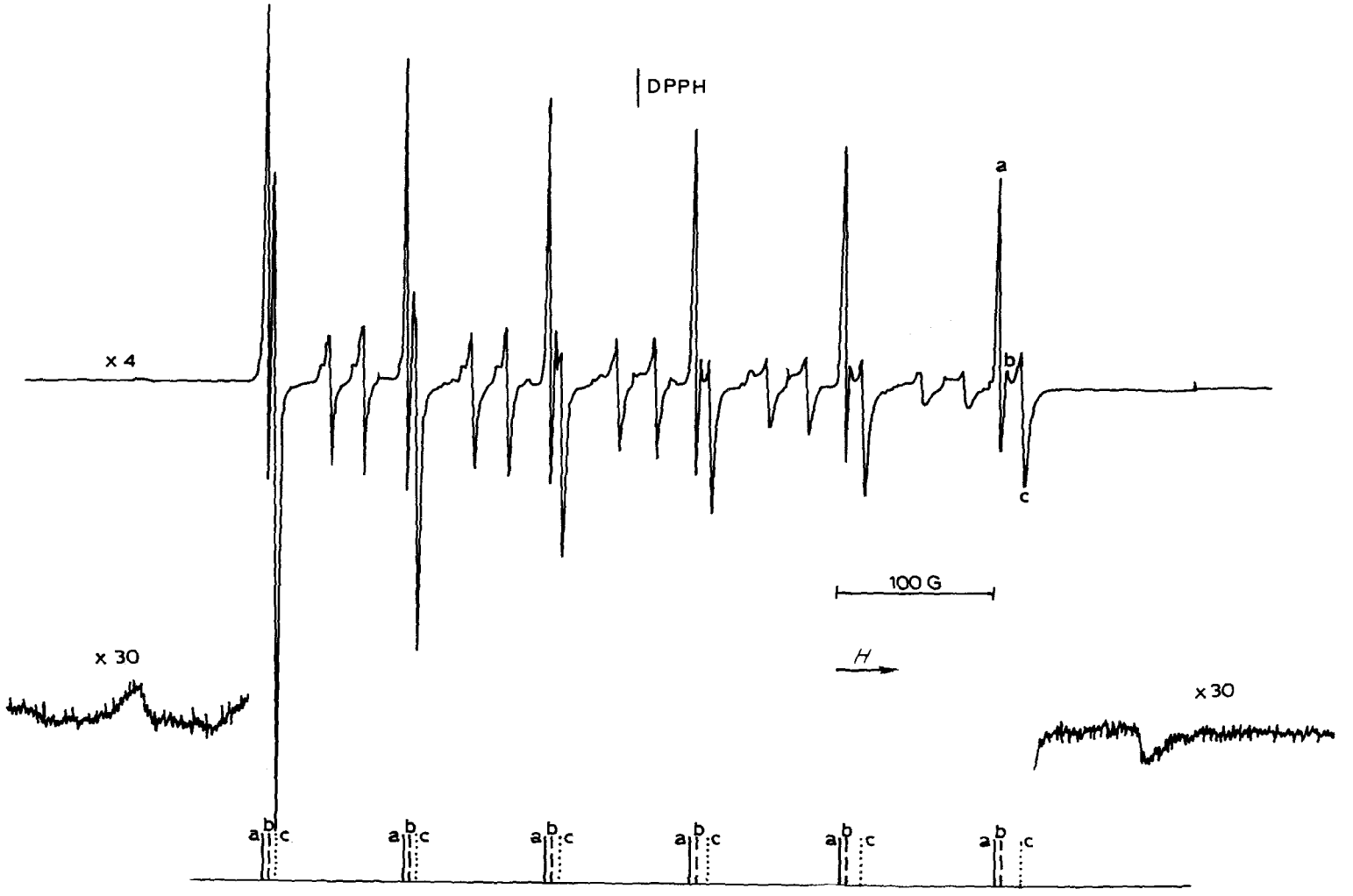

Figure 4 ESR spectrum of Mn^{2+} in calcite ex vaterite. Magnifications are with respect to the spectrum of Fig. 2.

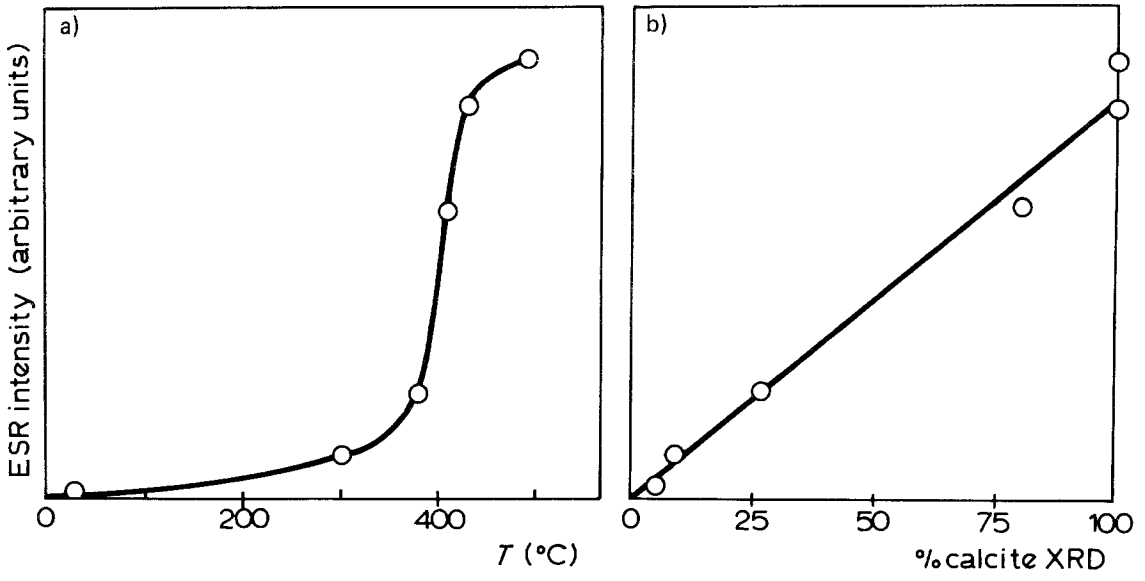

Figure 5 Intensity of the ESR spectrum of Mn^{2+} during the vaterite → calcite transformation as a function of (a) the temperature of thermal treatment and (b) the calcite percentage as determined by X-ray diffraction.

cite ex vaterite, and definitely much less intense than in the case of precipitated calcite;

(iii) the overall intensity of Vat 5 spectrum is only about 40% of that expected for precipitated calcite with 50 ppm Mn, as deduced from a comparison with the spectral intensitites for the 10 and 100 ppm Mn-containing calcite.

4. Discussion

The spin Hamiltonian appropriate for Mn^{2+} in a crystal with an axial field (such as calcite) [34–36] is

$$\mathcal{H} = g\beta H \cdot \hat{S} + D[\hat{S}_z^2 - \tfrac{1}{2}S(S+1)] + A\hat{S} \cdot \hat{I}. \quad (1)$$

The subscript "z" refers to the axial symmetry axis, D is the axial field parameter and A is the nuclear coupling constant. A and g are assumed to be isotropic. This Hamiltonian accounts satisfactorily for the spectrum of Mn^{2+} in calcite single crystals provided that one considers that there are two non-equivalent positions for the cations in the structure [22, 24, 29].

The spectrum of crushed calcite single crystals has been interpreted by Bleaney, Rubins and Abraham [37, 38] as follows. The resonance field for transitions other than $M = \frac{1}{2} \leftrightarrow M = -\frac{1}{2}$ varies very rapidly with the angle between the principal symmetry axis and the field. For this reason, transitions other than $M = \frac{1}{2} \leftrightarrow M = -\frac{1}{2}$ are almost smeared out in powdered specimens, where θ assumes a random value because of the random orientation of crystallites. Random orientation also causes signals to pile up at two particular θ values, namely $\theta = 90°$ and $\theta \approx 42°$. The central allowed sextuplet ($M = \frac{1}{2} \leftrightarrow M = -\frac{1}{2} : \Delta m = 0$) is therefore expected to split in powders into two sets of six lines. One set ($\theta = 90°$) shows a constant shift with respect to the unperturbed spectrum, i.e. the six hyperfine lines are equally spaced. The other set ($\theta \approx 42°$) shows a linear dependence of the position of the hyperfine lines upon m. This is more precisely seen from the relation for the energies of the levels concerned in the $M = \frac{1}{2} \leftrightarrow M = -\frac{1}{2}$ transition

$$E_{\pm\frac{1}{2}} = E^0_{\pm\frac{1}{2}}(A, m) \pm \frac{D^2 \sin^4\theta}{g\beta H} \pm \frac{D^2 \cos^2\theta \sin^2\theta}{g\beta H}\left(\frac{72\,Am}{g\beta H} - 8\right) \quad (2)$$

where $E^0_{\pm 1/2}$ are the energies of the unperturbed levels [39]. For $\theta = 90°$ the third term, which depends linearly upon m, vanishes whereas the second term introduces a constant shift. For $\theta \approx 42°$ the third term is non-vanishing. The spacing for all lines is, however, affected by second-order terms proportional to A^2/H, so that even for the case of $\theta = 90°$ some small increase of spacing with increasing field will occur.

4.1. ESR spectrum of Mn^{2+} in polycrystalline calcite

The above synopsis provides the basis for understanding the spectrum of Mn^{2+} in polycrystalline calcite shown in Fig. 2. The major feature is the sextuplet from the allowed ($\Delta m = 0$) transition $M = \frac{1}{2} \leftrightarrow M = -\frac{1}{2}$. The five pairs of lines between the intense lines of the sextuplet are the forbidden ($\Delta m = \pm 1$) transitions, well developed in this case because of the strong axial field [38]. The intense sextuplet lines are each composed of three components (designated "a", "b" and "c" in Fig. 2). The strong component "a", for which the spacing is only slightly dependent on field, is identified as the $\theta = 90°$ signal, whilst the strong component "c", which has an increased spacing indicating dependence both on H and on m, is identified as the $\theta \approx 42°$ signal. The weak component "b" has the same spacing characteristics as component "a", and can be accounted for by a third signal for which $\theta = 0°$. The above equation for $E_{\pm 1/2}$ shows that a signal with $\theta = 0°$ would not depend on m, but would exhibit a constant shift from the signal $\theta = 90°$, as observed. Whereas $\theta = 90°$ and $\theta \approx 42°$ signals arise as piling-up effects from the polycrystalline nature of the sample (but with D constant), the $\theta = 0°$ signal is explained by the occurrence of variable D values in the sample [39]. Line positions depend on D more strongly at $\theta = 90°$ than at $\theta = 0°$ [40], so the effect is to produce some broadening of the $\theta = 90°$ signal and to allow the $\theta = 0°$ signal to emerge distinctly. Such $\theta = 0°$ signals were observed by Barry and Lay [39] in Mn^{2+}-exchanged zeolites. It remains to comment on the weak lines present throughout the spectrum but which are most clearly manifested in the outer regions (magnified in Fig. 2). These correspond to the other $\Delta M = \pm 1$ transitions, namely, $M = \pm 5/2 \leftrightarrow \pm 3/2, \pm 3/2 \leftrightarrow \pm 1/2$ expected for the $Mn^{2+}\,{}^6S_{5/2}$ configuration, which are not completely smeared out. In contrast to the $M = \frac{1}{2} \leftrightarrow M = -\frac{1}{2}$ case, which is unsensitive to the two non-equivalent cation positions in the structure [22], these $\Delta M = \pm 1$ transitions may be split by this effect. It is of interest to note that the outer spectral lines (shown magnified in Fig. 2) are indeed split.

The most significant difference between the spectrum of Mn^{2+} in our polycrystalline calcite (surface area 25 to $30\,m^2\,g^{-1}$; $\bar{d} \sim 100\,nm$) and Mn^{2+} in crushed single crystals of calcite is the presence of the "b" component corresponding to $\theta = 0°$. As already indicated, this can be accounted for by heterogeneity in the value of the axial field parameter. We suggest that this is due to the small crystallite size, with many subsurface Mn^{2+} ions able to "feel" the truncating effect of a surface or the distorting effect of a crystal imperfection on the local coordination.

4.2. ESR spectrum of Mn^{2+} in polycrystalline vaterite

No structured signal due to Mn^{2+} in vaterite was observed. This closely resembles the result of Low and Zeira [30] who found no ESR spectrum of Mn^{2+} in aragonite at room temperature. However, they did find that a spectrum developed in aragonite on heating the solid. Their explanation was that manganese ions were present as Mn^{3+} in their mineral sample, but that reduction to Mn^{2+} occurred on heating. We regard an explanation based on the presence of Mn^{3+} as unlikely in our case, since special precautions were taken to avoid oxidation during preparation and no obvious source of electrons is available for reduction on heating. Moreover, there seems no good reason to expect Mn^{3+} in vaterite and not in calcite. No increase in our calcite ESR spectrum occurred when polycrystalline calcite was heated.

We consider that a more likely explanation for the non-appearance of a characteristic Mn^{2+} ESR spectrum in vaterite is that there is a very heterogeneous local co-ordination around the Mn^{2+} ions, leading to large variations of the axial field parameter D and smearing out of the signal. Compared to calcite, precipitated microcrystalline vaterite shows X-ray line broadening and lattice distortion [16]. Vaterite has a lower density, a higher entropy [15] and a lower crystal symmetry than calcite. The cation co-ordination with oxygen is especially relevant with respect to the replacement of Ca^{2+} by Mn^{2+}. In vaterite the co-ordination is distorted 8-fold cubic [11] as compared with 6-fold octahedral in calcite. The cation site is therefore larger in vaterite. The replacement of Ca^{2+} by Mn^{2+} in calcite is already adversely affected by the size disparity (Mn^{2+} is 20% smaller in radius than Ca^{2+}), and this will be further accentuated in vaterite. It is probable, therefore, that there will be a local adaptation of the oxygen environment when Mn^{2+} is placed in the 8-fold hole, but it is unlikely to be unique at all sites.

4.3. Transformation of vaterite to calcite

Vaterite is a metastable phase, so no transition point in the thermodynamic sense is expected. The conversion is a kinetically controlled process and therefore it is not surprising that samples prepared in different ways by different workers have led to different results. According to Rao [14] the activation energy is high ($> 360\,kJ\,mol^{-1}$), and this is indicative of a nucleation process. The sigmoid shape of Fig. 5a can be understood on this basis.

The inflection point (410° C) in Fig. 5a is close to the transition temperatures cited in previous work [12, 13]. Rao [14], however, states that the transformation is "immeasurably slow" at 450° C, but this is clearly incompatible with both our X-ray data (Fig. 1) and our ESR data (Fig. 5a). It may be argued that the presence of Mn^{2+} ions in the structure itself favours the transformation, in spite of the low concentration (50 ppm). However, this is ruled out by the linear relation shown in Fig. 5b. If Mn^{2+} acted as a nucleation centre for the transition, the intensity of the ESR spectrum of Mn^{2+} in calcite would develop more quickly in the initial stages than the X-ray pattern of the calcite structure. This is not the case. The percentage conversion estimated by ESR analysis is closely parallel to that estimated by X-ray analysis.

It remains to discuss the spectra of the vaterite samples before and after transformation to calcite. The spectrum of Vat 0 (Fig. 3) shows that the ESR technique is a sensitive indicator for calcite impurity. From the fact that the straight line in Fig. 5b passes through the origin one may infer that there is no enrichment of Mn^{2+} in the calcite phase. Taken together with the fact that Mn^{2+} in vaterite does not give a structured spectrum, this means that ESR in the presence of the Mn^{2+} probe is a very suitable way to follow the transformation.

The ESR method reveals information which is additional to that obtainable by X-ray diffraction in respect of the local site symmetry. All vaterite samples and also the sample of calcite ex vaterite exhibit differences from Mn^{2+} in precipitated calcite, showing that some features of the initial vaterite are not completely removed on conversion to calcite and annealing at 500° C. These features are: (i) a strong smearing out of all the fine structure due to the $M = \pm 5/2 \leftrightarrow \pm 3/2, \pm 3/2 \leftrightarrow \pm 1/2$ transitions, as evidenced by a comparison of the outer parts of the spectrum in Figs 2 and 4, respectively, (ii) a more intense "b" sextuplet in comparison with the "a" and "c" sextuplets (most easily seen in the central part of the spectrum), and (iii) an overall spectrum which although of the expected linewidth is less intense than in directly precipitated calcite. All of these features are attributable to small fluctuations in the axial field parameter D.

5. Conclusions

The work has shown that Mn^{2+} is a satisfactory ESR probe in monitoring crystallization during the growth of a new phase. The hyperfine structure reveals characteristics of the cation site symmetry in the resulting polycrystalline solid which are not detectable by X-ray analysis. The detail furthermore distinguishes between effects of multiple site symmetry and distortion and thereby acts as a fingerprint for the biography and origin of the crystals. The method should be capable of application also to chemical transformations and to crystallite growth in ionic materials of technological importance.

Acknowledgements

The authors thank Mr B. Chapman for assistance with the X-ray diffraction measurements and the Italian Consiglio Nazionale delle Ricerche (CNR) for a grant to one of us (BF).

References

1. H. J. MEYER, *Z. Kristallogr.* **121** (1965) 220.
2. Y. KITANO, *Bull Chem. Soc. Japan* **35** (1962) 1973 and 1980.
3. R. B. GAMMAGE and D. R. GLASSON, *Chem. Ind.* **35** (1963) 1466.
4. K. SIMKISS, *Nature* **201** (1964) 492.
5. J. L. BISCHOFF and W. S. FYFE, *Amer. J. Sci.* **266** (1968) 65.
6. J. L. BISCHOFF, *ibid.* **266** (1968) 80.
7. J. W. McCAULEY and R. ROY, *Amer. Min.* **59** (1974) 947.
8. J. D. C. McCONNELL, *Mineral Mag.* **32** (1960) 535.
9. S. R. KAMHI, *Acta Cryst.* **16** (1963) 770.
10. R. W. G. WYCKOFF, "Crystal Structures", Vol. 2 (Interscience, New York, 1964) p. 359.
11. H. J. MEYER, *Z. Kristallogr.* **128** (1969) 183.
12. G. LUCAS, *Bull Soc. Chim. Franc. Min.* **70** (1947) 185.
13. C. N. R. RAO and K. J. RAO in "Progress in Solid State Chemistry", edited by H. Reiss, Vol. 4 (Pergamon, Oxford, 1967) p. 131.
14. M. S. RAO, *Bull Chem. Soc. Japan* **46** (1973) 1414.
15. A. G. TURNBULL, *Geochim. Cosmochim. Acta.* **37** (1973) 1593.
16. D. O. NORTHWOOD and D. LEWIS, *Amer. Min.* **53** (1968) 2089.

17. J. TURKEVICH, S. LARACH and P. N. YOCOM, in "Reactivity of Solids", edited by G. M. Schwab (Elsevier, Amsterdam, 1965) p. 117.
18. K. N. SHRIVASTAVA and P. VENKATESWARLU, *Proc. Ind. Acad. Sci.* **64** (1966) 275.
19. G. BACQUET, S. DUGAS and C. ESCRIBE, *J. Solid State Chem.* **19** (1976) 251.
20. F. K. HURD, M. SACHS and W. D. HERSCHBERGER, *Phys. Rev.* **93** (1954) 373.
21. C. KIKUCHI, *ibid.* **100** (1955) 1243.
22. H. M. McCONNELL, *J. Chem. Phys.* **24** (1956) 904.
23. C. KIKUCHI and R. AGER, *Bull. Amer. Phys. Soc.* **2** (1958) 135.
24. C. KIKUCHI and L. M. MATARRESE, *J. Chem. Phys.* **33** (1960) 601.
25. L. M. MATARRESE, *ibid.* **34** (1961) 336.
26. R. A. SERWAY, *Phys. Rev. B.* **3** (1971) 608.
27. V. LUPEI, A. LUPEI and I. URSU, *ibid.* **6** (1972) 4125.
28. G. E. BARBERIS and R. CALVO, *Solid State Commun.* **15** (1974) 173.
29. G. E. BARBERIS, R. CALVO, H. G. MALDONADO and C. E. ZARATE, *Phys. Rev. B.* **12** (1975) 853.
30. W. LOW and S. ZEIRA, *Amer. Min.* **57** (1972) 1115.
31. P. H. KASAI, *J. Phys. Chem.* **66** (1962) 674.
32. H. P. KLUG and L. E. ALEXANDER, "X-ray Diffraction Procedures" (Wiley, New York, 1954) p. 410.
33. S. G. TULLETT, R. G. BOARD, G. LOVE, H. R. PERROTT and V. D. SCOTT, *Acta. Zool. (Stockholm)* **57** (1976) 79.
34. W. LOW, *Phys. Rev.* **101** (1956) 1827.
35. *Idem, ibid.* **105** (1957) 793.
36. *Idem,* "Paramagnetic Resonance in Solids" (Academic Press, New York, 1960).
37. B. BLEANEY and R. S. RUBINS, *Proc. Phys. Soc.* **77** (1961) 103.
38. A. ABRAHAM and B. BLEANEY, "Electron Paramagnetic Resonance of Transition Ions" (Clarendon Press, Oxford, 1970) p. 200.
39. T. I. BARRY and L. A. LAY, *J. Phys. Chem. Solids* **27** (1966) 1821.
40. R. C. BARKLIE and K. O'DONNELL, *J. Phys. C, Solid State Phys.* **10** (1977) 4127.

Received 19 November 1980 and accepted 18 February 1981.